



Exergetic, economic and environmental analysis of temperature controlled solar air heater system

Ali Etem Gürel^{a,b}, Gökhan Yıldız^{c,*}, Alper Ergün^d, İlhan Ceylan^d

^a Düzce University, Engineering Faculty, Department of Mechanical Engineering, Düzce, Turkey

^b Düzce University, Düzce Vocational School, Department of Electricity and Energy, Düzce, Turkey

^c Düzce University, Institute of Graduate Studies, Department of Mechanical Engineering, Düzce, Turkey

^d Karabük University, Technology Faculty, Department of Energy Systems Engineering, Karabük University, Karabük, Turkey

ARTICLE INFO

Keywords:

Solar energy
Exergy analysis
Energy analysis
Thermoeconomic analysis
Exergoeconomic analysis

ABSTRACT

Solar energy systems are widely utilized to obtain environmentally friendly and sustainable electrical and thermal energy that able to be used in many applications. Temperature-controlled solar air heater (SAH) system with a zigzag finned plate and flat plate was designed, manufactured, and tested experimentally in this study. It was determined that the set temperature was 15% higher than the flat plate SAH outlet temperature. The most important cause for this increase, the air is exposed preheating in the first collector. As the heat transfer surface area raised thanks to the zigzag fins in the second collector, the temperature of the air increases even more. SAH system's energy efficiency was found to be 71.15% on average. SAH system's maximum exergy efficiency was determined as 3.7%. The SAH system's average exergy destruction is calculated to be 651.58 W on average. According to the enviroeconomic analysis of the system, hourly CO₂ mitigation was found to be 1.04 kg CO₂/h and the environmental cost was 1.508 ¢/h. The energy cost was calculated as 0.0834 \$/kWh, while the exergoeconomic parameter was calculated as 0.1931 kWh/\$. In addition, the energy payback period was determined as 1.35 years, while the exergy payback period was determined as 45.9 years.

1. Introduction

Energy demand is increasing rapidly to meet the needs of domestic and industrial users in the world (Durakovic et al., 2020). Fossil fuels are used in more than 80% of the world's primary energy need to meet this energy demand (Bakay and Ağbulut, 2021). However, the biggest problem for fossil fuels is the increase in demand and their rapid depletion (Ceylan et al., 2021). At the same time, the use of fossil fuels has negative consequences on human health and the environment (Yıldız et al., 2020). In recent years, researchers have turned to clean and renewable energy sources due to these health and environmental problems (Khanlari et al., 2021). Therefore, the popularity of clean and renewable energy has increased recently (Abo-Elfadl et al., 2021). Solar energy, one of the unlimited, clean, and renewable energy sources, is widely used all over the world (Abuşka, 2018). Both thermal and electrical energy are obtained from solar energy (Tuncer et al., 2020). Thermal energy gained using solar radiation is widely used in different applications such as preheating, space heating, refrigeration, drying, greenhouse, and air conditioning (Ceylan and Gürel, 2016).

Solar thermal applications have a simple and cheap structure. Two types of solar collectors are commonly used in these applications. These; solar air heaters (SAH) and solar water heaters (SWH). SWHs can cost-effectively provide hot water for buildings or industrial needs (Şevik, 2014). Although the application areas of SAH are limited, the efficiency achieved in thermal applications is approximately three times more than the photovoltaic power production applications' efficiency. SAHs are preferred in low temperature applications because of their limited temperature interval. SAHs contribute to HVAC systems, drying systems, and cold storage systems (Qasem et al., 2020). Many scientists have tested different techniques to raise the SAH's efficiency. Some of these methods are fin design, slotted and filled absorbers, and baffles (Venkatesan and Senthil, 2020). The purpose of all these methods is to raise the heat transfer between the absorber plate and the air (Hu and Zhang, 2019).

Energy analysis is generally applied to analyze system performance in SAHs. There are many studies on energy analysis in SAHs. For example, Zhang et al. investigated a SAH's energy performance with the slot-perforated corrugated plate. It is expected that a slit-perforated corrugated plate increases the heat transfer area. It was emphasized

* Corresponding author.

E-mail address: gokhan81540@ogr.duzce.edu.tr (G. Yıldız).

<https://doi.org/10.1016/j.clet.2021.100369>

Received 2 April 2021; Received in revised form 14 December 2021; Accepted 20 December 2021

Available online 24 December 2021

2666-7908/© 2021 Published by Elsevier Ltd. This is an open access article under the CC BY license (<http://creativecommons.org/licenses/by/4.0/>).

| Nomenclature | | PCM | Phase change material |
|--------------|---|-------------------|------------------------------|
| SAH | Solar air heater | SV | Salvage value (\$) |
| I | Solar radiation (W/m^2) | TCI | Total cost investment (\$) |
| \dot{E}_x | Exergy (W) | SFF | Sinking fund factor |
| c_p | Specific heat ($\text{kJ/kg} \cdot ^\circ\text{C}$) | FAC | First annual cost (\$) |
| A | Area (m^2) | AMC | Annual maintenance cost (\$) |
| \dot{E} | Energy (W) | TCI | Total cost investment (\$) |
| \dot{E}_x | Exergy (W) | V | Air velocity (m/s) |
| T | Temperature ($^\circ\text{C}$) | n | Life time (year) |
| \dot{m} | Mass flow rate (kg/s) | Z | Economic parameter |
| m | Mass (g) | R_{ex} | Exergoeconomic parameter |
| ARC | Annual operating cost | φ | Environmental parameter |
| CE | Cost of electricity (\$/kWh) | Subscripts | |
| CRF | The capital recovery factor | in | Inlet |
| HVAC | Heating, ventilation and air conditioning | out | Outlet |
| SWH | Solar water heater | dest | Destruction |
| W_n | Uncertainties in the independent variables | c | Collector |
| w | Dimensional function | op | Operating |
| R | Uncertainty function | abs | Absorber |
| W_R | Total uncertainty | f | Fan |

that one of the most important parameters affecting system performance is the absorber plate height. The system efficiency reaches the highest value with 67.83%, when the air velocity in the collector reaches 1.14 m/s. SAH used in the study produced 820.7 MJ of heat during the heating season. This situation has the potential to reduce 43.1 kg of coal and 102.1 kg of CO_2 emissions environmentally (Zhang et al., 2018). Debnath et al. experimentally investigated SAH's performance in North East Indian climate. In this study, collector inclination angles, mass flow rate, two different absorber plates, and single and double glass parameters are taken into consideration. As a result, it was determined that the double-glazed absorber plate increases both energy and exergy efficiency. In addition, increasing mass flow rate is important parameters that increase energy efficiency. Efficiency increase varies between 10.35% and 17.42% with the enhancement in the number of glasses and mass flow rate. Corrugated plates' usage increased energy efficiency by 14% as it caused turbulent flow and increased the heat transfer area. Single glass SAH's exergy efficiency is 6.867% lower for 0.0118 kg/s mass flow rate compared with double glass SAH (Debnath et al., 2018). Perwez and Kumar analyzed the spherical dimple plate SAH and flat plate SAH's thermal performance in different environmental conditions in India. The experiments were carried out at a mass flow rate between 0.009 kg/s and 0.028 kg/s. The increment in the spherical dimple plate SAH's temperature was detected at 0.009 kg/s air mass flow rate approximately 4.6 $^\circ\text{C}$ higher than that of the flat plate SAH. At the same time, the spherical dimple plate SAH's thermal efficiency is higher than the flat plate SAH by 23.45%–35.50% (Perwez and Kumar, 2019). Deeyoko et al. analyzed the flat plate SWH's thermal performance. Square and rectangular fins were used to raise the thermal performance in this study. It was determined that the rectangular fin SWH gives more energy and exergy efficiency than the square fin SWH. It was determined that the rectangular fin SWH has a lower payback and energy payback period compared to the square fin SWH (Deeyoko et al., 2019). Kalaiarasi et al. experimentally performed flat plate SAH's energy and exergy analysis. The SAH has an absorber consisting of longitudinally welded copper strips. This structure has a heat storage system sensitive to copper pipes of high-quality synthetic oil. The studies were performed at air mass flow rate between 0.018 kg/s and 0.026 kg/s. Because of experiments, the obtained energy and exergy efficiencies varied between 49.4%–59.2% and 18.25%–37.53%, respectively, at 0.026 kg/s air mass flow rate in sensible heat storage SAH. Sensible heat storage

SAH outperformed the flat plate SAH without storage (Kalaiarasi et al., 2016).

Exergy analysis is different from energy analysis. Because, in this analysis, it is aimed to obtain more efficient systems by the system's reducing the inefficiencies. There are many studies on SAHs' exergy analysis. For example, Akpınar and Koçyiğit (2010) analyzed the SAH's performance, which has a flat plate without fins and different fins. Experiments were conducted at 0.0074 kg/s and 0.0052 kg/s air mass flow rate. All systems' energy efficiency varies between 20% and 82% while exergy efficiency varies between 8.32% and 44%. While the lowest efficient system was the flat plate SAH, the highest efficiency was SAH Type II (with leaf type). Experiment analyzes showed that SAH's efficiency depends upon solar radiation, the collectors' surface geometry, and airflow velocity (Akpınar and Koçyiğit, 2010). Bouadila et al. 2014 conducted a SAH's energy and exergy analysis with latent energy storage system with packed bed using phase change material (PCM) spherical capsules. The effects of solar radiation and airflow velocity on the system were tested. The daily energy efficiency changed between 32% and 45%, while the exergy efficiency changed between 13% and 25% (Bouadila et al., 2014). Sahu and Prasad conducted the SAH's exergy analysis with an arc-shaped wire ribbed roughened absorber plate. It was determined that the roughened SAH performed better than the flat plate SAH (Sahu and Prasad, 2016). Hanif et al. performed the flat plate SAH's energy and exergy efficiency analysis at different inclination angles (25°, 35°, and 50°) and different airflow rates (1.31, 2.11, 2.72 and 3.03 kg/s). The best performance values were obtained at 3.03 kg/s airflow rate and 35° inclination angle. The system's the total, maximum energetic and minimum exergy efficiency were determined as 71%, 51%, and 24%, respectively (Hanif et al., 2018). Ghiami and Ghiami performed the system's energy and exergy analysis in a SAH using paraffin wax as a PCM. SAH was tested at 0.017 kg/s, 0.014 kg/s and 0.009 kg/s air mass flow rates. The SAH's energy efficiency without PCM was determined as 14.30%, while the SAH's energy efficiency with PCM at 0.017 kg/s airflow rate was 26.78%. Exergy efficiency changed from 4.86% to 20.47% in all operating conditions (Ghiami and Ghiami, 2018). Kumar and Layek conducted the system's energy and exergy analysis using rib roughness bent on an absorber plate in a SAH. As a result, the thermal, effective and exergetic efficiency was 1.81, 1.79, and 1.81 times better than the normal absorber plate SAH, respectively (Kumar and Layek, 2019). Saravanakumar et al., using Matlab software,

performed optimization, exergy and energetic analysis of SAH with plate and fins. The SAH's maximum exergy efficiency was determined as 5.2% in optimum conditions with eight fins and 0.012 kg/s air mass flow rate (Saravanakumar et al., 2020). Abuşka and Şevik conducted a comparative experimental study between two SAHs with flat and grooved absorber bases. Because of the experiments, it was observed that grooved SAH has higher energy efficiency than the SAH with flat plate. The SAH's average exergy efficiency was determined to vary between 6% and 12%. Environmental economic cost was between 4.5 \$ and 5.77 \$ per year for traditional and modified SAH, respectively. The exergy and thermal efficiency of V-grooved and flat SAH were found to be 6%–12% and 43%–60%, respectively. In addition, it was determined that the average payback period is 4.3 and 4.6 years (Abuşka and Şevik, 2017). Sari et al. performed exergy analysis using baffles and delta fins to increase the SAH's efficiency. SAH was analyzed experimentally and numerically. As a result, the maximum exergy efficiency was obtained as 30.44% in the SAH with baffles and delta fins (Sari et al., 2020).

In this study, the SAH's exergy, economic and environmental analysis were focused. According to the literature, many studies were presented to examine the energy and exergy performances of SAHs. However, it is necessary to evaluate not only the energy and exergy performances of SAHs but also economically and environmentally. However, the number of studies in which SAHs are evaluated economically and environmentally is insufficient. In this respect, this study is important to provide information in this area. Moreover, one of the innovative aspects of this study is that the SAH system has flat plate collector and zigzag finned plate collector. The flat plate collector acts as a preheater in the SAH system. The heated air is passed through the zigzag fins collector to raise surface area of heat transfer, thus increasing the air temperature more. Another innovative aspect of the system is that it is a temperature-controlled system. Heat transfer in the system increases with the usage of different absorber plates in SAH systems. In this way, it is expected that the system's energy and exergy efficiency will increase. Because of obtaining higher yields from SAH, it is expected to reach lower amounts economically. More suitable economic and environmental results can be obtained in direct proportion to the use of lower cost equipment in the system. The energy and exergy payback times of SAHs were also calculated in this study. The study's flow chart is given in Fig. 1.

2. Materials and methods

2.1. Experimental setup

In present study, a temperature-controlled SAH with flat plate and zigzag finned was experimentally analyzed. The experimental setup is shown in Fig. 2.

There are two different design solar collectors in the SAH system. The first of these collectors has flat plate absorber and initially, outside air passes the system from this collector. The air is heated in the flat plate SAH and then goes to the zigzag finned plate SAH. In the structure of the second collector, zigzag design was used to allow the heated air to come into contact with the larger surface area. The air coming out of this collector is sent to the place to be heated with the help of a fan. The SAH system's one of the most important properties is the temperature control. The temperature sensor located at the fan output sends the measured temperature from the determined point to the process controller. The process controller transmits this received data to the inverter. The inverter checks the fan speed according to the set temperature. If the air temperature to be sent to the environment decreases below the set temperature, the inverter reduces the fan speed and tries to reach the set temperature. The inverter increases fan speed and decreases the temperature, when the air temperature to be sent to the environment starts to increase above the set temperature. The set temperature expression defines the outlet temperature of zigzag finned SAH. The technical properties of the measurement devices and components used in this system are shown in Table 1.

2.2. Uncertainty analysis

The experimental study's total uncertainty value was determined by the following equations. In the equation, W_R is the study's total uncertainty (%), R and w are the uncertainty function and the dimensional coefficient, respectively (Saridemir et al., 2021). W_n expresses the uncertainties in the independent variables in the same equation (Cingiz et al., 2021).

$$W_R = \left[\left(\frac{\partial R}{\partial x_1} w_1 \right)^2 + \left(\frac{\partial R}{\partial x_2} w_2 \right)^2 + \dots + \left(\frac{\partial R}{\partial x_n} w_n \right)^2 \right]^{1/2} \quad (1)$$

The total uncertainty is 0.68% for the SAH system.

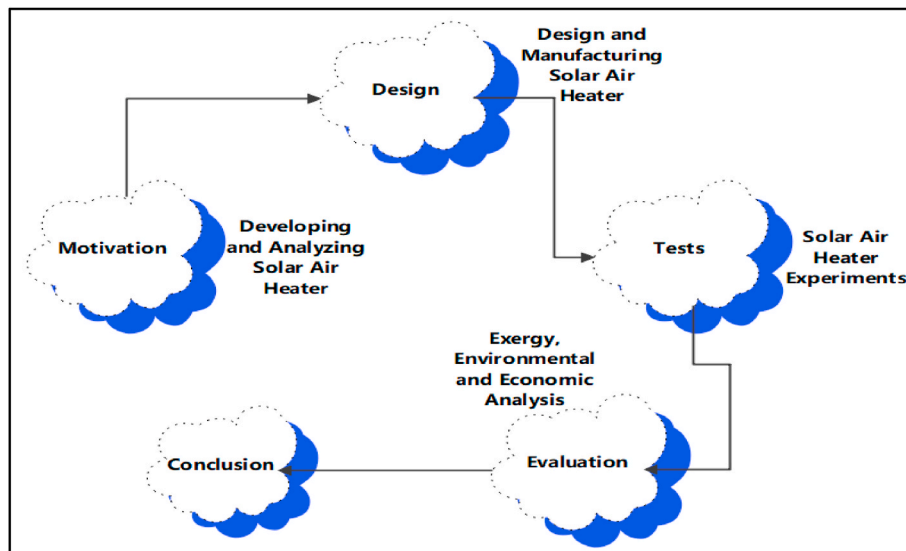


Fig. 1. The present study's flow chart.

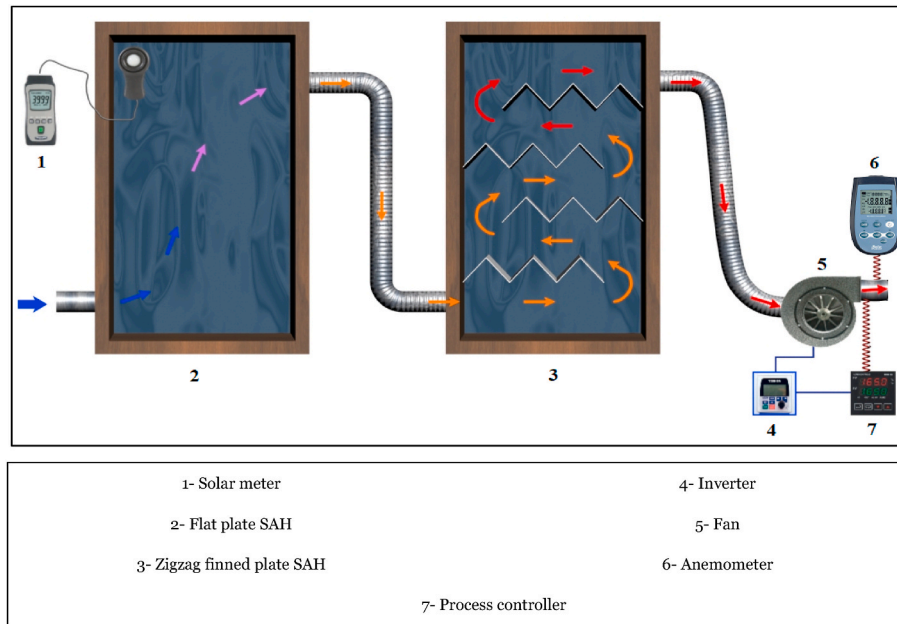


Fig. 2. View of the experimental setup.

Table 1

Technical properties of measurement devices and components in this study.

| Equipment | Technical properties |
|---------------------------|--|
| Thermocouples | K Type, Temperature range: -10 to $+60$ °C Accuracy: ± 0.4 °C |
| Anemometer | Measurement range: 0.6 – 20 m/s Accuracy: ± 0.2 m/s |
| Inverter | AC Frequency Inverter for 0.75 kW 230 V |
| Process controller | 100 – 240 VAC or 24 VDC, Transmitter supply output, Analog output ($0/4$ – 20 mA, $0/2$ – 10 V), Transmitter supplement, PID control, Auto-tuning |
| Digital solar power meter | Measurement range: 0 – 2000 W/m ² Accuracy: $\pm 0.5\%$ W/m ² |

2.3. Theoretical analysis

2.3.1. Energy analysis

The energy rate from the system is given as follow:

$$\dot{E}_{out} = m \cdot c_p \cdot (T_{set} - T_{in}) \quad (2)$$

The energy's rate obtained from the sun and fan is calculated as follow:

$$\dot{E}_{in} = (I \cdot A) + \dot{W}_f \quad (3)$$

The energy efficiency is given in Eq. (4).

$$\eta_{en} = \frac{\dot{E}_{out}}{\dot{E}_{in}} \quad (4)$$

2.3.2. Exergy analysis

Exergy analysis is of great importance in systems that generate thermal energy and rely on the thermodynamics' second law (Ergün, 2020). The SAH system's exergy balance equation can be shown as (Gürel et al., 2020):

$$\sum \dot{E}x_{in} - \sum \dot{E}x_{out} - \sum \dot{E}x_{dest.} = dEx_{system} / dt \quad (5)$$

If the system is considered as steady, it can be written as following Eq. (5).

$$\sum \dot{E}x_{in} - \sum \dot{E}x_{out} = \sum \dot{E}x_{dest.} \quad (6)$$

Here, $\dot{E}x_{in}$, $\dot{E}x_{out}$, and $\dot{E}x_{dest.}$ are exergy input, exergy output, and exergy destruction, respectively.

Total exergy entering the system in Eq. (6) $\dot{E}x_{in}$ is exergy's sum obtained from the solar radiation and the inlet air's exergy. The atmosphere's energy is infinite but its exergy is zero. Since the input of the SAH system is taken directly from the atmosphere, it is not possible to talk about a work potential at this point. Thus, the exergy entering can only be expressed as exergy from solar radiation, and this expression was defined by (Petela, 2003) as follows.

$$\dot{E}x_{in} = \dot{E}x_{sun} = \left[1 - \frac{4}{3} \left(\frac{T_0}{T_{sun}} \right) + \frac{1}{3} \left(\frac{T_0}{T_{sun}} \right)^4 \right] \cdot I \cdot A_c \quad (7)$$

In the equation, the sun's surface temperature (T_{sun}) is considered to be 5777 K.

The output exergy gained or the exergy gained by the fluid where the SAH temperature increases from T_0 to T_{air} is given in Eq. (8).

$$\dot{E}x_{out} = \dot{m} \cdot c_{pair} \left[(T_{set} - T_0) - T_0 \ln \left(\frac{T_{set}}{T_0} \right) \right] \quad (8)$$

Besides, the SAH system's exergy efficiency is as follows (Ahmadian and Schmidt, 2020):

$$\eta_{ex} = \frac{\dot{E}x_{out}}{\dot{E}x_{in}} \quad (9)$$

2.3.3. Economic analysis

Annual operating cost (ARC) is calculated as follows (Hassan and Abo-Elfadl, 2018):

$$ARC = (\dot{m} \Delta P / \rho) t_{op} CE \quad (10)$$

where ΔP is the pressure drop in the system, ρ is the air density, t_{op} operating time and CE is the electricity cost.

The capital recovery factor (CRF) is given by (Kumar and Layek, 2019):

$$CRF = \frac{i(1+i)^n}{(1+i)^n - 1} \quad (11)$$

where, n is the assumed the SAH system's service life of 20 years (Hassan et al., 2021), i is the annual interest assumed to be 10% (Abd Elbar et al., 2019). The first annual cost (FAC) is calculated as follow:

$$FAC = CRF \times TCI \quad (12)$$

where TCI is total cost investment. The sinking fund factor (SFF) is given by:

$$SFF = \frac{i}{(1+i)^n - 1} \quad (13)$$

The annual salvage value (ASV) is described as follow:

$$ASV = SFF \times SV \quad (14)$$

$$SV = 0.12 \times TCI \quad (15)$$

Here, SV represents the scrap price and was taken as %12.

Annual maintenance cost (AMC) is assumed to be 10% of the first annual cost (Saravanakumar et al., 2020).

$$Annual\ Cost\ (AC) = FAC + AMC + ARC - ASV \quad (16)$$

The SAH system's annual useful energy is determined as follows:

$$Annual\ Useful\ Energy = I_{average} \times A_{abs.} \times \eta_{SAH} \times SD_{approximately} \times h_{op} \quad (17)$$

Here, $I_{average}$ is the total solar radiation's average on the SAH system's tilted surface, $A_{abs.}$ is the absorber area, η_{SAH} is the SAH system's efficiency, the $SD_{approximately}$ represent the approximate sunny days' number and h_{op} operating hours per day.

2.3.4. Energy payback time

Important parameters are always used to compare the applicability of renewable energy systems. EPBT hinges on the energy and the annual energy output from the system (Hassan et al., 2021). $(EPBT)_{en}$ and $(EPBT)_{ex}$ equations are as follow:

$$(EPBT)_{en} = \frac{E_{in}}{E_{out}} \quad (18)$$

$$(EPBT)_{ex} = \frac{E_{in}}{\dot{E}x_{out}} \quad (19)$$

2.3.5. Exergoeconomic analysis

Exergoeconomic analysis is an economic analysis technique related to exergy. Traditional cost analysis is combined with exergy analysis to improve the energy systems' performance (Sahota and Tiwari, 2017). In this analysis, the aim is to predict the optimum cost structure, optimum cost values in this analysis, and make it easy for designers to find ways to effectively increase the system's performance. Traditionally, the exergoeconomic parameter is calculated as exergy loss per unit cost to minimize the loss (Hassan et al., 2021). Therefore, the SAH system's exergoeconomic parameter $R_{g, ex}$ is calculated as follows:

$$R_{g, ex} = \frac{\dot{E}x_{out}}{AC} \quad (20)$$

Here, $\dot{E}x_{out}$, $R_{g, ex}$, and AC are the annual exergy output, the exergoeconomic parameter, and the annual cost, respectively.

2.3.6. Enviroeconomic analysis

In this study, the environmental assessment is based on the CO_2 emission rate to the environment. Since the SAH system is a renewable energy source, it reduces CO_2 emissions that pose a great danger to the environment. The average CO_2 emission in the environment is around $980\text{ gCO}_2/\text{kWh}$ for electricity production from coal in the power plant. However, considering the transmission losses due to the distribution losses of 20% and the inefficiency of the electrical equipment of 40%, this value becomes $2\text{ kgCO}_2/\text{kWh}$. For this reason, the CO_2 mitigation of

the SAH system every year is calculated as follows (Gürel et al., 2020):

$$\varphi_{CO_2} = \frac{(En_{out} \times n) \times 2}{1000} \quad (21)$$

Here, φ_{CO_2} is defined as the environmental parameter in tons, n is the SAH system's lifetime and En_{out} as the annual energy output. The environmental economic approach defines the CO_2 mitigations' annual revenue over the SAH system's lifetime (Caliskan et al., 2012). The environmental economic parameter is as in Eq. (22) shown below (Tripathi et al., 2016):

$$Z_{CO_2} = z_{CO_2} \times \varphi_{CO_2} \quad (22)$$

Here, Z_{CO_2} is the environmental economic parameter and z_{CO_2} is the international carbon price, which is considered to be 14.5 \$ per ton of CO_2 (Gaur and Tiwari, 2014).

3. Result and discussions

SAH system's the exergy efficiency and solar radiation are given according to the daily hour in Fig. 3. Solar radiation varies between 482 and 930.2 W/m^2 . The SAH system's average exergy efficiency was observed as 2.21%. Additionally, the maximum exergy efficiency was determined to be 3.7%, when solar radiation was as 911.5 W/m^2 in 220 min. In addition, the set temperature at this moment is the highest temperature recorded as 54.2°C . Considering these values, it is seen that the set temperature and solar radiation are important in enhancement of exergy efficiency. Although solar radiation reached higher values throughout the experiment, there was no point at which set temperature exceeded 54.2°C . This situation brings the exergy efficiency of the set temperature close to high values although there is less solar radiation. As a result, it clearly shows that other variables have to be considered together for SAH systems.

Inlet to flat plate collector and set temperatures (after the fan) are shown in Fig. 4. As stated before, in this study, flat plate and zigzag fin plate SAHs are operated together. For this reason, preheating is accomplished in the flat plate SAH. The heated air from the flat plate SAH was circulated through the zigzag finned plate SAH, increasing the temperature of the air. The important point to be considered here is that the fan speed increases as the air temperature rises above the set temperature between 110 and 390 min. This is the period when radiation and ambient temperature are reasonably high in this range. However, SAH temperatures remained limited because of the increase in fan speed. In the study, the set temperature was determined as minimum 37.5°C , maximum 54.2°C and SAH inlet temperature minimum 28.3°C , maximum 33.6°C . During the experiments, while the average set temperature was 48.59°C , the collector's average inlet temperature was determined as 31.23°C . The collector inlet temperature and the set temperature were increased by an average of 55.6%.

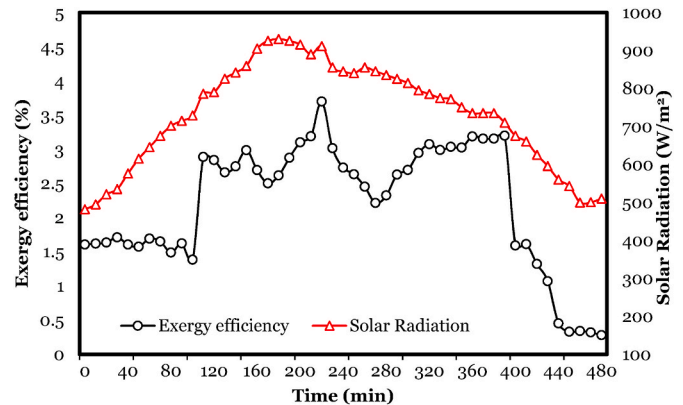


Fig. 3. Changes in exergy efficiency and solar radiation.

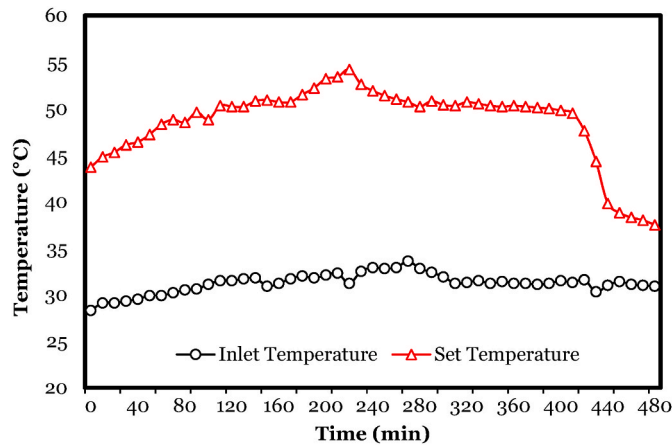


Fig. 4. Time-dependent changes of temperature values.

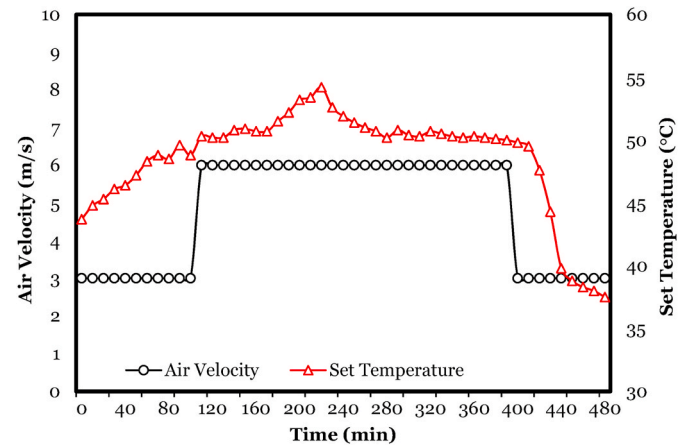


Fig. 6. Changes in set temperature and air velocity.

Exergy destruction and set temperature are shown in Fig. 5. Exergy destruction varies between 463.88 W and 825.21 W. As seen in Fig. 5, the highest exergy destruction was determined as 825.21 W in 180 min. The set temperature corresponding to this exergy destruction is 51.5 °C. Exergy destruction is 799.81 W at 54.2 °C, which is the highest set temperature. As can be seen from these values, temperature and exergy destruction are not directly related. However, in 180 min, when the exergy destruction is the highest, the highest solar radiation is 930.2 W/m². Exergy destruction is related to the amount of solar radiation.

As mentioned in the previous sections, one of the SAH design's the most important features is temperature control. As seen in Fig. 6, if the air temperature exceeds the set temperature, fan speed is changed by the inverter. Thus, the temperature can be held at the set temperature. The air temperature was set to 50 °C in this study. Since the air temperature rises above 50 °C in 110 min, the air velocity, which is 3 m/s, was increased to 6 m/s by the inverter to reduce the temperature. SAH system was able to reduce the increasing air temperature below 50 °C only in 390 min. It is not as easy as expected to reduce the increasing air temperature. This shows how important temperature control is.

Average performance values of the SAH system are given in Table 2. In present study, the exergy inlet varies between 439.50 and 847.40 W, and the exergy outlet varies between 1.31 and 30.71 W. The exergy loss in SAH changes between 432.44 and 825.21 W. The exergoeconomic and enviroeconomic values of the SAH system are given in Table 3.

4. Conclusion

In this paper, SAH system's exergy, environmental and economic analyzes with flat plate and zigzag fin plate was performed together. The system's first and second law efficiency analyzes were made. In addition, SAH system's the economic and environmental analyzes were made.

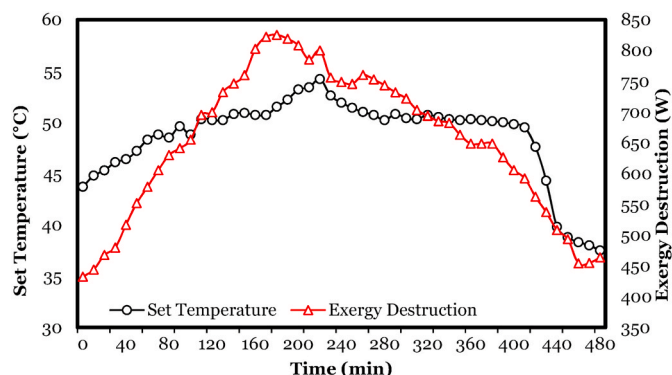


Fig. 5. Changes of set temperature and exergy destruction.

Table 2

Average performance values of SAH system.

| I (W/m ²) | T_{in} (°C) | T_{set} (°C) | Ex_{in} (W) | Ex_{out} (W) | Ex_{dest} (W) | η_{ex} (%) | η_{en} (%) |
|-------------------------|---------------|----------------|---------------|----------------|-----------------|-----------------|-----------------|
| 732.29 | 31.23 | 48.59 | 667.21 | 15.62 | 651.58 | 2.21 | 71.15 |

Table 3

Exergoeconomic and enviroeconomic parameters of SAH system.

| φ_{CO_2} (kgCO ₂ /h) | Z_{CO_2} (€/h) | Energy cost (\$/kWh) | $R_{g,ex}$ (kWh/\$) | $(EPBT)_{en}$ (y) | $(EPBT)_{ex}$ (y) |
|---|------------------|----------------------|---------------------|-------------------|-------------------|
| 1.04 | 1.508 | 0.0834 | 0.1931 | 1.35 | 45.9 |

Accordingly, the theoretical and experimental observations in the study are as follows:

- Two different SAHs are used in the system, namely flat plate, and zigzag fin plate. Considering these SAHs as a whole, their performances have been investigated experimentally. According to the results of this study, it was seen that the ambient air's average temperature could be improved by 55.6% by using the SAH system. The fan speed increased after a certain period and this limited the temperature increase.
- The SAH system's average exergy efficiency is 2.21%. A raise in exergy efficiency was observed because of reaching the optimum outlet temperature and solar radiation for the SAH system.
- The SAH system's average energy efficiency was calculated as 71.15%.
- The SAH system's average exergy destruction was calculated as 651.8 W. The increase for the radiation has a very high share in the increase for exergy destruction. Because, according to the data obtained during the experiments, the highest exergy destruction occurred in 180 min, which is the highest solar radiation.
- Enviroeconomic analysis results of the SAH system have determined hourly CO₂ mitigation as 1.04 kgCO₂/h and environmental cost as 1.508 €/h.
- According to the SAH system's economic analysis results, the energy cost was found to be 0.0834 \$/kWh, while the exergoeconomic parameter was calculated as 0.1931 kWh/\$.
- The energy payback time was determined as 1.35 years, while the exergy payback period was determined to be 45.9 years.

5. Limitation and challenges

There are many studies on increasing the system efficiency of SAHs.

However, some limitations and difficulties need to be resolved in SAH applications. These limitations and challenges are noted below:

- The amount of heat transfer is low because of the air's low heat transfer properties used in SAHs.
- There is a need to transport large volumes of air because of the low air density.
- Because of the low air thermal capacity, it cannot be used as a storage fluid. Additional material is required for energy storage.
- The costs of SAHs can be high without proper design.

In addition to the many positive performances of SAH usage, the above-mentioned problems limit the system to operate more efficiently. Therefore, it is important to rise the number of studies to overcome these limitations and challenges.

6. Future works

According to the experience and research in this study, the following suggestions for improving the performance of SAH systems can be considered for future studies:

- The use of symmetrically arranged PCM on the absorber plate in SAHs increases the air's heat absorption. Paraffin wax is widely used in energy storage applications. Other types of energy storage materials should be tried as PCM. In addition, studies should be conducted to investigate the full and PCM's homogeneous melting. In this way, PCM will be used efficiently.
- With the use of reflectors, it is ensured that the reflected sun rays are collected again in solar energy systems. As in many solar energy systems, the usage of reflectors in SAHs can be used to increase the system's efficiency. The quantity of more detailed studies on reflector SAH systems should be increased.
- Energy payback time and environmental benefits can be achieved if production, operation, and maintenance costs are lower, as well as obtaining different configurations to enhance the SAHs' efficiency. The economic viability of the collector materials must be sustainable.
- It is still difficult to achieve the required temperature in SAHs because of heat loss and blower cost. Therefore, experimental and numerical analyzes should be performed to determine the optimum values of the raggedness elements and shape configurations on the absorber surface.
- Nanomaterials increase the surface area and act as thermal storage material, as in many applications (Yildiz et al., 2021). Nanofluids, which are widely used in energy and solar energy systems, can also be used in SAHs. The effect of coating SAHs absorbers with black paint mixed with nanomaterials on thermal efficiency should be investigated for different nanomaterials and fractions.
- Optimization techniques such as response surface method, genetic algorithm, and stochastic iterative perturbation technique can be used to predict the SAH's energy and exergy efficiencies.

Declaration of competing interest

The authors declare that they have no known competing financial interests or personal relationships that could have appeared to influence the work reported in this paper.

References

- Abd Elbar, A.R., Yousef, M.S., Hassan, H., 2019. Energy, exergy, exergoeconomic and enviroeconomic (4E) evaluation of a new integration of solar still with photovoltaic panel. *J. Clean. Prod.* 233, 665–680.
- Abuşka, M., Şevik, S., 2017. Energy, exergy, economic and environmental (4E) analyses of flat-plate and V-groove solar air collectors based on aluminium and copper. *Solar Energy* 158, 259–277.
- Abo-Elfadl, S., Yousef, M.S., El-Dosoky, M.F., Hassan, H., 2021. Energy, exergy, and economic analysis of tubular solar air heater with porous material: an experimental study. *Applied Thermal Engineering* 196, 117294.
- Abuşka, M., 2018. Energy and exergy analysis of solar air heater having new design absorber plate with conical surface. *Appl. Therm. Eng.* 131, 115–124.
- Ahmadian, E., Schmidt, R.R., 2020. Exergy analysis of district energy systems and comparison of their exergetic, energetic and environmental performance. *Int. J. Exergy* 32 (2), 103–129.
- Akpınar, E.K., Koçyiğit, F., 2010. Energy and exergy analysis of a new flat-plate solar air heater having different obstacles on absorber plates. *Appl. Energy* 87 (11), 3438–3450.
- Bakay, M.S., Ağbulut, Ü., 2021. Electricity production based forecasting of greenhouse gas emissions in Turkey with deep learning, support vector machine and artificial neural network algorithms. *J. Clean. Prod.* 285, 125324.
- Bouadila, S., Lazaar, M., Skouri, S., Kooli, S., Farhat, A., 2014. Energy and exergy analysis of a new solar air heater with latent storage energy. *Int. J. Hydrogen Energy* 39 (27), 15266–15274.
- Caliskan, H., Dincer, I., Hepbasli, A., 2012. Exergoeconomic, enviroeconomic and sustainability analyses of a novel air cooler. *Energy Build.* 55, 747–756.
- Ceylan, İ., Gürel, A.E., 2016. Solar-assisted fluidized bed dryer integrated with a heat pump for mint leaves. *Appl. Therm. Eng.* 106, 899–905.
- Ceylan, İ., Gürel, A.E., Ergün, A., Ali, İ.H.G., Ağbulut, Ü., Yıldız, G., 2021. A detailed analysis of CPV/T solar air heater system with thermal energy storage: a novel winter season application. *J. Build. Eng.* 42, 103097.
- Deeyoko, L.A.J., Balaji, K., Iniyan, S., Sharmela, C., 2019. Exergy, economics and pumping power analyses of flat plate solar water heater using thermal performance enhancer in absorber tube. *Appl. Therm. Eng.* 154, 726–737.
- Cingiz, Z., Katircioğlu, F., Sarıdemir, S., Yıldız, G., Çay, Y., 2021. Experimental investigation of the effects of different refrigerants used in the refrigeration system on compressor vibrations and noise. *International Advanced Researches and Engineering Journal* 5 (2), 152–162.
- Debnath, S., Das, B., Randive, P.R., Pandey, K.M., 2018. Performance analysis of solar air collector in the climatic condition of North Eastern India. *Energy* 165, 281–298.
- Durakovic, B., Yıldız, G., Yahia, M.E., 2020. Comparative performance evaluation of conventional and renewable thermal insulation materials used in building envelopes. *Tehnicki vjesnik-Technical Gazette* 27 (1), 283–289.
- Ergün, A., 2020. Energy and exergy analysis of a PV/thermal storage system design integrated with nano-enhanced phase changing material. *Int. J. Exergy* 32 (1), 82–101.
- Gaur, A., Tiwari, G.N., 2014. Exergoeconomic and enviroeconomic analysis of photovoltaic modules of different solar cells. *Journal of Solar Energy* 2014, 1–8.
- Ghiami, A., Ghiami, S., 2018. Comparative study based on energy and exergy analyses of a baffled solar air heater with latent storage collector. *Appl. Therm. Eng.* 133, 797–808.
- Gürel, A.E., Ağbulut, Ü., Ergün, A., Yıldız, G., 2020. Energy, exergy, and environmental (3E) assessments of various refrigerants in the refrigeration systems with internal heat exchanger. *Heat Tran. Res.* 51 (11), 1029–1041.
- Hanif, M., Khattak, M.K., Khan, M., Ramzan, M., Abdurab, 2018. Energy, exergy and efficiency analysis of a flat plate solar collector used as air heater. *Sains Malays.* 47 (5), 1061–1067.
- Hassan, H., Abo-Elfadl, S., 2018. Experimental study on the performance of double pass and two inlet ports solar air heater (SAH) at different configurations of the absorber plate. *Renew. Energy* 116, 728–740.
- Hassan, H., Yousef, M.S., Abo-Elfadl, S., 2021. Energy, exergy, economic and environmental assessment of double pass V-corrugated-perforated finned solar air heater at different air mass ratios. *Sustain. Energy Technol. Assessments* 43, 100936.
- Hu, J., Zhang, G., 2019. Performance improvement of solar air collector based on airflow reorganization: a review. *Appl. Therm. Eng.* 155, 592–611.
- Kalaiaarasi, G., Velraj, R., Swami, M.V., 2016. Experimental energy and exergy analysis of a flat plate solar air heater with a new design of integrated sensible heat storage. *Energy* 111, 609–619.
- Khanlari, A., Sözen, A., Afshari, F., Tuncer, A.D., Ağbulut, Ü., Yilmaz, Z.A., 2021. Numerical and experimental analysis of parallel-pass forced convection solar air heating wall with different plenum and absorber configurations. *Int. J. Numer. Methods Heat Fluid Flow*. <https://doi.org/10.1108/HFF-03-2021-0160>.
- Kumar, A., Layek, A., 2019. Energetic and exergetic performance evaluation of solar air heater with twisted rib roughness on absorber plate. *J. Clean. Prod.* 232, 617–628.
- Perwez, A., Kumar, R., 2019. Thermal performance investigation of the flat and spherical dimple absorber plate solar air heaters. *Solar Energy* 193, 309–323.
- Petela, R., 2003. Exergy of undiluted thermal radiation. *Solar Energy* 74 (6), 469–488.
- Qasem, N.A., Arnous, M.N., Zubair, S.M., 2020. A comprehensive thermal-hydraulic assessment of solar flat-plate air heaters. *Energy Convers. Manag.* 215, 112922.
- Sahota, L., Tiwari, G.N., 2017. Energy matrices, enviroeconomic and exergoeconomic analysis of passive double slope solar still with water based nanofluids. *Desalination* 409, 66–79.
- Sahu, M.K., Prasad, R.K., 2016. Exergy based performance evaluation of solar air heater with arc-shaped wire roughened absorber plate. *Renew. Energy* 96, 233–243.
- Saravanakumar, P.T., Somasundaram, D., Matheswaran, M.M., 2020. Exergetic investigation and optimization of arc shaped rib roughened solar air heater integrated with fins and baffles. *Appl. Therm. Eng.* 175, 115316.
- Sari, A., Sadi, M., Sabet, G.S., Mohammadi, M., Mohammadi, H., 2020. Experimental analysis and exergetic assessment of the solar air collector with delta winglet vortex generators and baffles. *J. Therm. Anal. Calorim.* 1–19.
- Sarıdemir, S., Yıldız, G., Hanedar, E., 2021. Effect of diesel-biodiesel-methanol blends on performance and combustion characteristics of diesel engine. *Düzce Üniversitesi*

- Bilim ve Teknoloji. Dergisi 9 (1), 189–201. <https://doi.org/10.29130/dubited.763009>.
- Şevik, S., 2014. Experimental investigation of a new design solar-heat pump dryer under the different climatic conditions and drying behavior of selected products. *Solar Energy* 105, 190–205.
- Tripathi, R., Tiwari, G.N., Dwivedi, V.K., 2016. Overall energy, exergy and carbon credit analysis of N partially covered photovoltaic thermal (PVT) concentrating collector connected in series. *Solar Energy* 136, 260–267.
- Tuncer, A.D., Khanlari, A., Sözen, A., Gürbüz, E.Y., Şirin, C., Gungor, A., 2020. Energy exergy and enviro-economic survey of solar air heaters with various air channel modifications. *Renew. Energy* 160, 67–85.
- Vengadesan, E., Senthil, R., 2020. A review on recent developments in thermal performance enhancement methods of flat plate solar air collector. *Renew. Sustain. Energy Rev.* 134, 110315.
- Yıldız, G., Çalış, B., Gürel, A.E., Ceylan, İ., 2020. Investigation of life cycle CO₂ emissions of the polycrystalline and cadmium telluride PV panels. *Environmental Nanotechnology, Monitoring & Management* 14, 100343.
- Yıldız, G., Ağbulut, Ü., Gürel, A.E., 2021. A review of stability, thermophysical properties and impact of using nanofluids on the performance of refrigeration systems. *Int. J. Refrig.* 129, 342–364.
- Zhang, H., Ma, X., You, S., Wang, Y., Zheng, X., Ye, T., Zheng, W., Wei, S., 2018. Mathematical modeling and performance analysis of a solar air collector with slit-perforated corrugated plate. *Solar Energy* 167, 147–157.